

H-induced plastic deformation of Gd thin films studied by STM

A. Pundt

Institute of Materials Physics, University of Göttingen, D-37073 Göttingen, Germany

M. Getzlaff and M. Bode

Institute of Applied Physics and Microstructure Research Center, University of Hamburg, D-20355 Hamburg, Germany

R. Kirchheim

Institute of Materials Physics, University of Göttingen, D-37073 Göttingen, Germany

R. Wiesendanger

Institute of Applied Physics and Microstructure Research Center, University of Hamburg, D-20355 Hamburg, Germany

(Received 20 July 1999; revised manuscript received 5 November 1999)

Surface modification of thin Gd films during hydrogen absorption has been investigated on the nanometer scale by scanning tunneling microscopy. Two different types of surface pattern appear that can be attributed to hydrogen-induced plastic deformation processes within the Gd film. Disklike islands are formed first due to GdH_2 precipitation and concomitant emission of extrinsic dislocation loops. At a later stage ramps appear on the surface as a result of glide displacements originating from misfit dislocations at the interface between the substrate and the thin film.

Studies of hydrogen in thin films have attracted considerable interest recently for a variety of reasons;¹⁻⁵ among other things, these are modifications of material properties, which are interesting from the point of view of basic physics (e.g., the metal-insulator transition⁶) and industrial applications (e.g., hydrogen-switchable mirrors⁷). Hydrogen absorption in thin films can produce an extremely high out-of-plane expansion due to the clamping of the thin film to the substrate.⁴ Yang *et al.* showed that within the solid solution phase the expansion can be predicted by linear elastic theory,⁸ and Laudahn *et al.* found⁹ this to be true for the stress. However, deviations from linear elastic theory were reported for high H concentrations due to the onset of plastic deformation in the film.^{9,10}

Two different processes have been proposed for plastic deformation and stress relaxation in thin Nb films.^{9,10} The first is the emission of extrinsic dislocation loops during hydride precipitation as observed experimentally in bulk material.¹¹ The second process is the glide of dislocation segments that originate from misfit dislocations in the vicinity of the interface between the film and the substrate.¹² The strain energy of the film increases during hydrogen absorption since the misfit between the adhering film and the substrate increases with H concentration. Thus, above a certain H concentration the formation of a misfit dislocation is favored energetically.

In this paper we present results of the effect of hydrogen loading on the topography of thin epitaxial films using *in situ* scanning tunneling microscopy (STM). Cover layers were avoided in order to follow the surface development of Gd during hydrogen exposure. Cover layers are frequently applied to protect the film surface from oxidation. The sample preparation and STM analysis were performed in an ultra-high vacuum (UHV) system with a base pressure in the low 10^{-11} mbar regime. The Gd(001) films were deposited onto

a W(110) crystal that was cleaned by heating in oxygen and flashing up to 2600 K. During Gd deposition from an *e*-beam evaporator the pressure remained below 3×10^{-10} mbar. Further details about the preparation procedure are described elsewhere.¹³ The measurements were performed immediately after sample preparation to ensure that the initial hydrogen concentration in the Gd film was low and the Gd film remained in the solid solution phase of the Gd-H system. The topography was measured with a commercial STM with cut Pt/Ir tips in the constant-current mode. The samples were dosed incrementally by admitting high purity hydrogen (99.999%) to a pressure of 1×10^{-7} mbar. The amount of hydrogen exposure is given in langmuir ($1 \text{ L} = 10^{-6} \text{ Torr s}$). After each adsorption step the chamber was reevacuated. All STM measurements were performed at room temperature.

From scanning tunneling spectroscopy it is known that atomically clean and well-ordered Gd(001) exhibits a pronounced surface state in the electronic structure.¹⁴ After hydrogen adsorption the surface state disappears and a significant decrease in the differential conductivity occurs. This means that the hydrogen-covered areas of the sample appear lower in the STM images recorded in the constant-current mode. Figure 1 shows a Gd(0001) surface after hydrogen exposures of 5 L (a), 10 L (b), and 20 L (c,d). The topography reflects the symmetry of the (0001)-oriented epitaxial Gd film with a thickness of about 10 nm: the steps of the terraces lie in $\langle 11\bar{2}0 \rangle$ directions and subtend 60° angles. Due to the epitaxial growth of the Gd film on W(110) only one grain occurs. After 20 L exposure (c) only a small area remains free of hydrogen and since this area still has the Gd surface state it appears slightly higher. In the following STM image [Fig. 1(d)], which is taken 40 min later, the elevated area has increased. The vanishing and reappearance of the Gd surface state on the *same* terrace is indicated by white

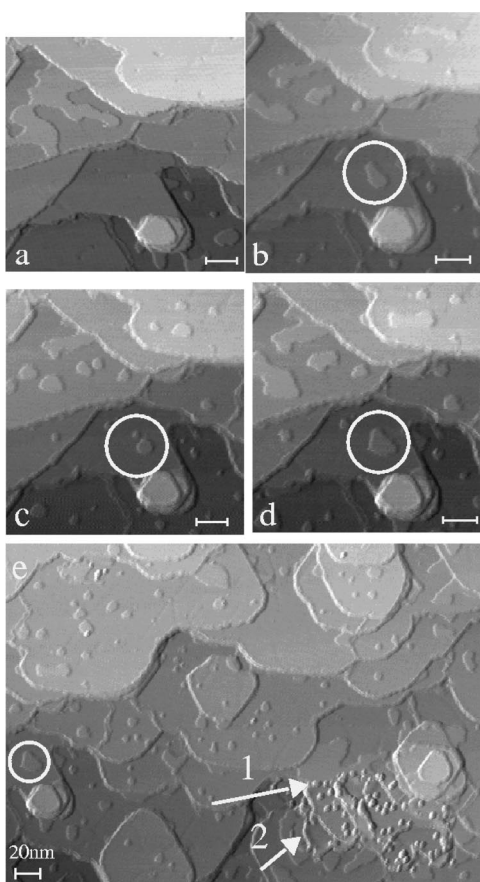


FIG. 1. STM images of a Gd(0001) film after total hydrogen exposures of 5 L (a), 10 L (b), and 20 L (c,d); all bars represent 20 nm. The Gd surface state is detectable as areas appearing higher on the *same* terrace in (a) whereas in (c) it almost disappeared. It reappears after 40 min, as can be seen in (d), indicating the removal of hydrogen from the surface. After 20 L, two different types of surface pattern appear (e): small islands with disklike shape (1) and ramps (2).

circles in Figs. 1(b)–1(d). It can be seen by a shrinking and growing of the apparently higher areas. The reappearance of the Gd surface state means that hydrogen has been removed from the Gd surface. Hydrogen has a large negative heat of solution in rare earth metals so it dissolves in interstitial sites even at very low gas pressures.¹⁵ Thus we conclude that the hydrogen that was at the surface has diffused into the interior of the film.

After an exposure of 20 L the surface topography changes in certain areas. Figure 1(e) shows such a location of the sample; the circle marks the same area as the circle in Fig. 1(d). Two different features were observed: (1) a large number of disklike islands and (2) occasionally ramp-shaped features. The disklike islands have a diameter of 35 Å and a height of about 3 Å [see Fig. 2(c)]. The patterned area appears to be rough compared to the smooth Gd or H/Gd surface on each terrace and is induced by the surface modification discussed below. The height profiles show that the edges of the island have steep steps. A height profile taken along the sloped region of a ramp is shown in Fig. 2(b). The line scan is taken from the left. The steep step occurs at the left side. The inclination extending from the step to the right covers several nanometers until it reaches the base level.

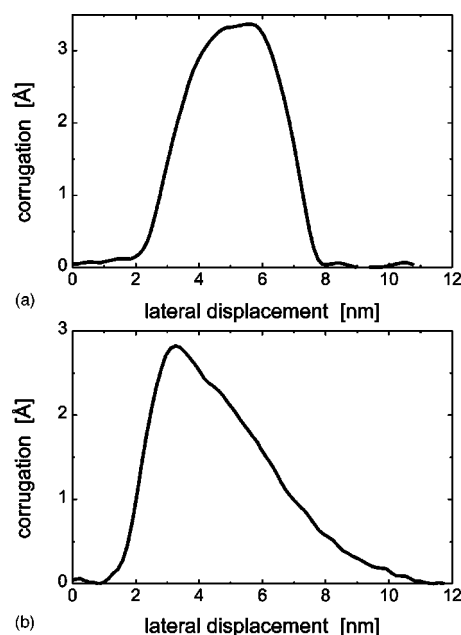


FIG. 2. Height profiles of (a) small disklike islands showing steps at their sides, and (b) a ramp, taken perpendicularly to the straight line. Here a steep step is followed by an inclination over several nanometers to the base level. Note the different scales for lateral displacement and corrugation.

Both islands and ramps are elevated [by about the distance of the (0001) planes] compared to the level of the Gd terrace and, therefore, are generated by *local material transport to the surface*.

The ramps only appear in regions where disklike island formation has taken place. The ramps seem not to originate from chains of close packed disklike islands since such an elevation should result in a step at all borderlines, as shown in Fig. 2(a). In contrast, a level inclination was found on one side and a step on the other side. Thus the two surface patterns have a different origin.

In the case of bulk Nb,¹¹ the volume increase during hydride precipitation is released by transporting surplus atoms into less stressed regions by emission of extrinsic dislocation loops. The local volume increase per Gd atom is about 12%. Misfit stress in $\langle 0001 \rangle$ directions is twice as large as in $\langle 11\bar{2}0 \rangle$ directions because of the anisotropy of the system. In a quantitative treatment this anisotropy has to be taken into account. During hydride precipitation misfit stress appears both in plane and out of plane. In the case of clamped thin films the emission of dislocation loops results in an in-plane and out-of-plane stress release, as shown schematically in Fig. 3(a). As soon as an emitted dislocation loop reaches the film surface it can be locally detected by an additional layer of atoms and corresponds to the observed disklike islands. It should be noted that a surface hydride cannot explain the disklike islands because it would appear deeper compared to the base level in the STM image. We attribute the disklike islands to localized hydride formation in the underlying Gd film.

To verify this interpretation the average hydrogen concentration can be estimated by measuring the relative amounts of disklike islands containing patterned area and unchanged surface area, which give the hydride volume (with about 1.8

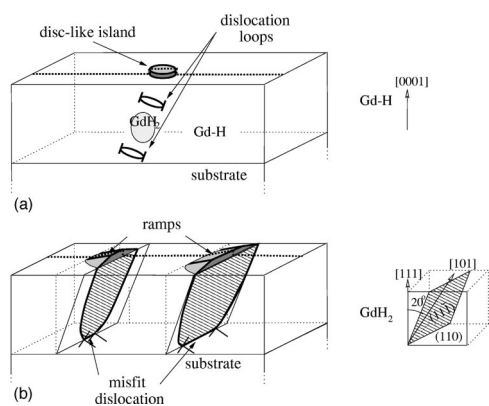


FIG. 3. (a) Schematic drawing of the model proposed for disk-like island formation. During internal hydride precipitation the surplus atoms are emitted in extrinsic dislocation loops and form islands. (b) Schematic drawing of the process proposed for ramp formation for the orientation of the analyzed Gd films. The in-plane stress-releasing 60° -misfit dislocation near the interface to the substrate is connected to the surface via a mixed-type dislocation line. At the surface such a dislocation line results in an elevated area above the edge dislocation. An atomic step appears where the $(11\bar{1})$ glide plane crosses the film surface. Height profiles along the broken lines can be compared with results of Fig. 2.

H/Gd) and the α -phase volume (with about 0.3 H/Gd), respectively. In the case of the STM image taken a total exposure of 20 L [Fig. 1(c,d)] this estimate leads to an average value of 0.08 H/Gd. An upper estimate for the hydrogen concentration in the Gd film at this stage [Fig. 1(c,d)] can be given by assuming that all exposed gaseous hydrogen (20 L) is absorbed by the 35 monolayers of Gd. This yields a maximum estimated hydrogen concentration of 1.14 H/Gd, which is well inside the two-phase field. Because the sticking coefficient is less than unity the true concentration is lower, consistent with the average value obtained above. Thus, the inhomogeneous hydrogen distribution inside the film, as expected within the two-phase region.

Further hydrogen exposure results in a spreading out of the patterned areas that contain islands and ramps, as presented in Figs. 4(a) and 4(b). We correlate the disk- and ramp-covered areas with the presence of the GdH_2 phase in the film. It should be noted that we identify the disklike islands with the emission of dislocation loops that are generated in Gd-H solid solution surrounded by GdH_2 precipitates. The ramps, however, occur in areas that consist only of GdH_2 .

According to the level rule the volume fraction of the GdH_2 phase increases with increasing total hydrogen content in the two-phase region.¹⁶ After high H exposure the spreading out of the elevated areas covers the whole analyzed region, representing the high hydrogen concentration within the whole Gd film. The spread contains two different features: first, new disklike islands and ramps appear. Second, the existing ramps elongate predominantly in the direction of the rim (cf. Fig. 3). Heavy H exposure leads to a surface pattern consisting almost exclusively of straight lines. They lie in $\langle 11\bar{2}0 \rangle$ directions of the as-prepared film, as shown in Fig. 4(c).

Since new ramps occur inside the regions where the un-

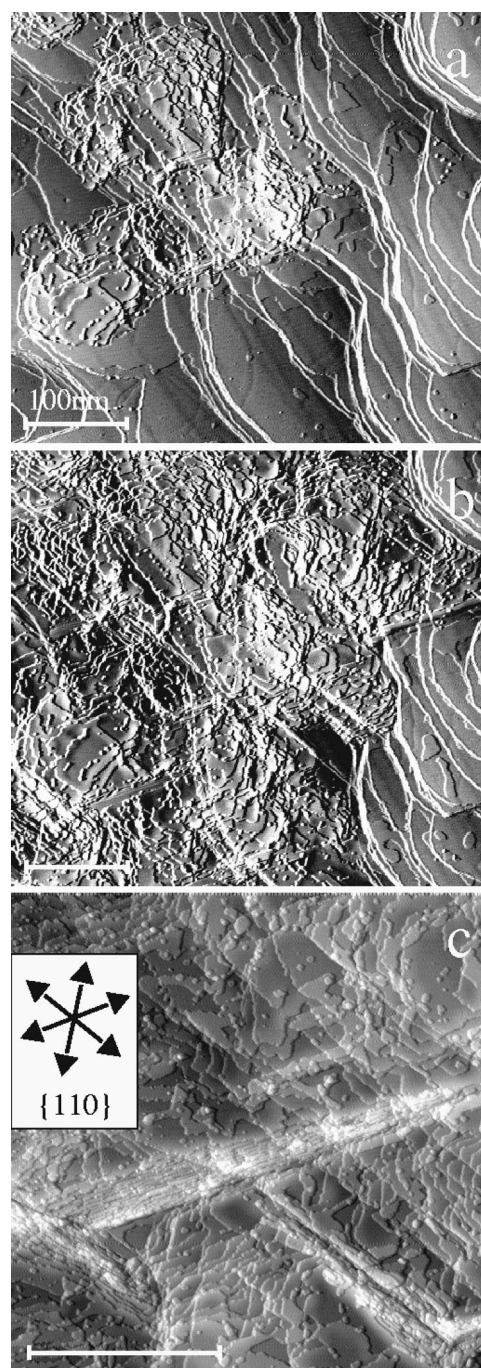


FIG. 4. STM images of the Gd surface after a hydrogen exposure of (a) 80 L and (b) 200 L. Further hydrogen exposure results in a spread of the localized surface pattern. After more than 3000 L (c) the whole surface is covered with straight lines that predominantly occur oriented to $\langle 110 \rangle$ fcc GdH_2 lattice directions, the former $\langle 11\bar{2}0 \rangle$ hcp Gd-H lattice directions. The right part of the area shown in (c) coincides with the upper left corner in (a) and (b).

derlying film is GdH_2 , they cannot be attributed to the misfit stress that appear at the GdH_2 -Gd interface. However, they can be related to high local in-plane stress between the GdH_2 film and the substrate. With regard to the bulk phase diagram, GdH_2 possesses fcc structure.¹⁷ In the following it is assumed that the former hcp lattice of Gd transforms into the fcc lattice of GdH_2 by changing the stack sequence of densest packed planes and, therefore, $\langle 11\bar{2}0 \rangle$ axes (hcp) are par-

allel to $\langle 110 \rangle$ (fcc).

The ramps can be interpreted by the formation of stress releasing dislocations. Two appropriate dislocations are shown schematically in Fig. 3(b) for the specific orientation of our GdH_2 film. The dislocation (drawn as a bold line) reduces in-plane misfit stress as soon as its glide plane is inclined to the normal vector of the interface. In the fcc lattice the $\{111\}$ planes are glide planes with $\langle 110 \rangle$ glide directions. The marked dislocation with a Burgers vector of $(1/2)\langle 110 \rangle$ which corresponds to a 60° -misfit dislocation, possesses an angle of $19^\circ 68'$ to the interface normal. Therefore, it can release in-plane stress. The area where glide occurred is hatched in Fig. 3(b). It is surrounded by three different parts: First, one part that is close to the interface and corresponds to an edge-type misfit dislocation; second, two parts that extend from the interface to the surface which are predominantly screw type dislocation; third, the rim of the ramp. It corresponds to the glide step on the surface. For thin films this type of dislocation has been proposed before,¹² but our measurements cannot determine whether the dislocation is formed on the surface and glides toward the interface, or vice versa.

The dislocation line is expected to have a high mobility in its glide plane. Gliding of the predominantly screw-type sections in $\langle 110 \rangle$ directions on $\{111\}$ planes leads to an elongation of the misfit dislocation near the interface. This is accompanied by an extension of the rim of the ramp. While the moving dislocation line passes, the local bonds between Gd atoms and the neighboring atoms reform and the atom rows move toward the surface. Following the $(11\bar{1})$ glide plane to the surface results in an atomic step on one side and a slope toward the other side and ramp enlarges. This is shown in Fig. 3(b).

The sloped region of the ramp is assumed to meet the original level at a position where the underlying $(11\bar{1})$ glide plane intersects with the interface, i.e., at the position of the misfit dislocation. Since the angle between the $(11\bar{1})$ plane and the surface is constant, the raised area depends on the distance between the surface and the dislocation line. Assuming a maximum distance of 10 nm for the $d=10$ nm

thick Gd film, a slope field expansion of $\Delta=3.4$ nm is obtained, using $d \sin(19^\circ 68')=\Delta$. This is in good agreement with the experimental findings shown in Fig. 2(b) where the raised area extends over about 5 nm (this is additional evidence for the dislocation mechanism proposed in this study).

At higher hydrogen concentrations the elongation of ramps along the rims leads to further stress release. As dislocation glide occurs in $\{111\}$ glide planes, glide steps on the surface form along $\langle 110 \rangle$ directions. In the STM images this elongation results in the straight lines that cover the whole film after heavy hydrogen exposure. The angles between these lines are 60° , as can be seen in Fig. 4(c), as expected for $\{111\}$ planes of a fcc lattice intersecting a (111) surface. To conclude, ramp and island formation verifies that plastic deformation of the film occurs during hydrogen absorption.

The STM measurements have shown that during hydrogen loading of thin epitaxial Gd films surface patterns develop above a critical concentration. Two different types were found: disklike islands and ramps. These surface patterns can be well described by two plastic deformation processes in the films that lead to glide steps on the film surface. First the emission of dislocation loops during hydride precipitation occurs, and secondly misfit dislocations form near the film-substrate interface. Since plastic deformation leads to stress release we suggest that a lot of thin metal films that are clamped to a substrate relax plastically after reaching a certain hydrogen-induced stress that corresponds to a critical hydrogen concentration. Overall, combining the ability of preparing high-quality epitaxial thin films with a detailed analysis of the mechanical properties during hydrogen absorption may lead to a deeper fundamental understanding of hydrogen-switchable thin films. It may also improve their industrial applications.

The authors would like to thank H. Teichler for stimulating discussions and R. L. Johnson for a critical reading of the manuscript. Financial support by the Deutsche Forschungsgemeinschaft via Sonderforschungsbereich 345, Grant Nos. Ki 230/19 and Wi 1277/4, as well as the Graduiertenkolleg "Physik nanostrukturierter Festkörper," is gratefully acknowledged.

¹P. F. Miceli, H. Zabel, and J. E. Cunningham, *Phys. Rev. Lett.* **54**, 917 (1985); P. F. Miceli and H. Zabel, *ibid.* **59**, 1224 (1987).

²A. Abromeit *et al.*, *J. Alloys Compd.* **253**, 58 (1997).

³F. Stillesjö, B. Hjörvarsson, and H. Zabel, *Phys. Rev. B* **54**, 3079 (1996).

⁴G. Song *et al.*, *Phys. Rev. Lett.* **79**, 5062 (1997).

⁵Ch. Rehm *et al.*, *Physica B* **234**, 483 (1997).

⁶R. Griessen *et al.*, *J. Alloys Compd.* **253**, 44 (1997).

⁷J. N. Huiberts *et al.*, *Nature (London)* **380**, 281 (1996).

⁸Q. M. Yang *et al.*, *Phys. Rev. B* **54**, 9131 (1996).

⁹U. Laudahn *et al.*, *J. Alloys Compd.* (to be published).

¹⁰U. Laudahn, Ph.D. thesis, Cuvillier Verlag Göttingen, 1998.

¹¹T. Schober, *Scr. Metall.* **7**, 1119 (1973); B. J. Makenas and H. K. Birnbaum, *Acta Metall.* **28**, 979 (1980).

¹²W. D. Nix, *Metall. Trans. A*, **20**, 2217 (1989).

¹³M. Getzlaff, M. Bode, and R. Wiesendanger, *Surf. Sci.* **410**, 189 (1998).

¹⁴M. Bode, M. Getzlaff, and R. Wiesendanger, *Phys. Rev. Lett.* **81**, 4256 (1998).

¹⁵Y. Fukai, *The Metal-Hydrogen System*, Vol. 21 of *Springer Series in Materials Science*, edited by U. Gonser (Springer-Verlag, Berlin, 1993).

¹⁶B. J. Beaudry and F. H. Speeding, *Metall. Trans. B* **6**, 419 (1975).

¹⁷*Binary Alloy Phase Diagrams*, edited by T. B. Massalsky (American Society for Metals, Metals Park, OH, 1990).